Hydrogen bonds in liquid water are broken only fleetingly

J. D. Eaves*†‡, J. J. Loparo*†, C. J. Fecko*§, S. T. Roberts*, A. Tokmakoff*¶, and P. L. Geissler**

*Department of Chemistry and George R. Harrison Spectroscopy Laboratory, Massachusetts Institute of Technology, Cambridge, MA 02139; and **Department of Chemistry, University of California, and Physical Biosciences and Material Sciences Divisions, Lawrence Berkeley National Laboratory, Berkeley, CA 94720

Although it is widely accepted that the local structure of liquid water has tetrahedral arrangements of molecules ordered by hydrogen bonds, the mechanism by which water molecules switch hydrogen-bonded partners remains unclear. In this mechanism, the role of nonhydrogen-bonded configurations (NHBs) between adjacent molecules is of particular importance. A molecule may switch hydrogen-bonding partners either (*i*) through thermally activated breaking of a hydrogen bond that creates a dangling hydrogen bond before finding a new partner or (*ii*) by infrequent but rapid switching events in which the NHB is a transition state. Here, we report a combination of femtosecond 2D IR spectroscopy and molecular dynamics simulations to investigate the stability of NHB species in an isotopically dilute mixture of HOD in D_2O. Measured 2D IR spectra reveal that hydrogen-bonded configurations and NHBs undergo qualitatively different relaxation dynamics, with NHBs returning to hydrogen-bonded frequencies on the time scale of water's fastest intermolecular motions. Simulations of an atomistic model for the OH vibrational spectroscopy of water yield qualitatively similar 2D IR spectra to those measured experimentally. Analysis of NHBs in simulations by quenching demonstrates that the vast majority of NHBs are in fact part of a hydrogen-bonded well of attraction and that virtually all molecules return to a hydrogen-bonding partner within 200 fs. The results from experiment and simulation demonstrate that NHBs are intrinsically unstable and that dangling hydrogen bonds are an insignificant species in liquid water.

femtosecond 2D IR spectroscopy | molecular dynamics | liquids

On average, molecules in liquid water are tetrahedrally coordinated but appear to engage in 10% fewer hydrogen bonds than in ice. Support for this estimate comes broadly, from latent heats of melting and vaporization, from x-ray and neutron scattering, and in very detailed form from molecular dynamics (MD) simulations (1–3). The role of nonhydrogen-bonded configurations (NHBs) in water's rapidly changing structure remains uncertain, lying at the heart of differences between mixture and continuum models of water (1, 3–8). Implicitly or explicitly, the interpretation of many experiments and MD simulations conceives of NHBs as broken or dangling hydrogen bonds, stable species that interconvert with a hydrogen-bonded configuration (HB) at a rate determined by the free energy barrier separating them. But it is also possible that NHBs are intrinsically unstable species that appear transiently during natural fluctuations about a hydrogen bond or when molecules trade hydrogen-bonding partners. These two scenarios not only provide qualitatively different interpretations of water's structure and how it evolves, but also imply different pictures for how water mediates chemical and biological processes. We have distinguished between these scenarios by using a combination of femtosecond 2D IR spectroscopy and MD simulations, finding that NHBs are inherently unstable, reforming hydrogen bonds on the time scale of water's fastest intermolecular motions.

The OH stretching vibration of an HOD molecule in D_2O is particularly sensitive to the hydrogen bonding environment of the proton. The absorption spectrum of the OH stretch peaks at a frequency several hundred wavenumbers lower than in the gas phase, with a breadth ($260 \, \text{cm}^{-1}$) reflecting a diverse distribution of microscopic environments. MD simulations confirm the expectation that the high-frequency (blue) side of the spectrum represents HOD molecules that interact weakly with their available hydrogen-bonding partner, whereas those involved in strong hydrogen bonds absorb at lower (red) frequencies (9–12). Femtosecond spectroscopies that probe the time evolution of the OH stretching frequency, ω_{OH}, for selected groups of molecules therefore provide a glimpse of changing HBs (12–19).

Fig. 1A quantifies the ability of ω_{OH} to discriminate between HB and NHB species. The plotted distributions were obtained from MD simulations with a conventional geometric criterion for detecting hydrogen bonds (12). They establish relative probabilities of HBs and NHBs but do not indicate the time scale or mechanism of interconversion. Indeed, many dynamical scenarios are consistent with these static results. Fig. 1 B and C illustrates 2D free energy surfaces representing such pictures (1). In either case trajectories spanning the vertical coordinate involve switching of hydrogen-bonding partners, but they differ fundamentally through the presence or absence of a barrier separating HBs from NHBs. In Fig. 1B, a free energy barrier separates HB from a stable NHB state, and switching trajectories may dwell in a region where the OH group lacks a hydrogen-bond acceptor. In Fig. 1C NHB is instead an unstable species, appearing fleetingly as the system traverses the transition-state region. Conceptually, one could distinguish between these two scenarios by observing how frequency distributions prepared in different regions of these free energy surfaces evolve in time. The presence of a barrier between NHB and HB implies a separation of time scales for fast fluctuations within basins of attraction and for crossing the barrier between them. If this scenario were accurate, the persistence time of molecules prepared in the NHB state should exceed the time scale of an orientational or translational hydrogen-bonding fluctuation, typically <200 fs (20, 21). By contrast, if NHB species exist only transiently, a frequency distribution prepared on the blue side would relax to line center on this time scale.

2D IR spectroscopy probes the stability of NHB species by measuring the time development of OH oscillators that initiate from HB and NHB environments. Analogous to the COSY experiment in NMR, 2D IR spectroscopy is a Fourier transform technique that uses an excitation sequence of femtosecond IR pulses with variable time delays. A 2D IR correlation spectrum, displayed as a function of two frequency axes (ω_1 and ω_3), is

---

CHEMISTRY

Fig. 1. Frequency probability distribution calculated from MD simulation and two free energy surfaces describing the breaking and reforming of hydrogen bonds consistent with this probability distribution. (*A*) Equilibrium distribution of ω_{OH} computed from MD simulations (solid green line). Geometrical criteria (see text) discriminate HB (solid red line) from NHB (solid blue line) contributions to the total distribution. The fractional population of NHB (dotted black line) increases sharply with ω_{OH}. (*B* and *C*) Two possible chemical scenarios for NHBs in water and the connection to IR spectroscopy. In *B*, NHBs are broken hydrogen bonds that are entropically stabilized. The yellow arrow illustrates how molecules in this picture trade hydrogen bonds. An initially HB molecule enters NHB and resides there before thermal agitation pushes it over the barrier into a hydrogen bond with another partner. In *C*, NHB is not a stable species but a transition state that trajectories pass through as they switch hydrogen-bonding partners (yellow solid line). (*B* and *C Upper*) The free energy along the ω_{OH} coordinate that is identical for either scenario.

closely related to the joint probability that a molecule has an initial excitation frequency ω_1 and arrives at a target frequency ω_3 after waiting a time τ_2. The 2D IR spectrum has a positive peak corresponding to the fundamental transition ($v = 1 \leftarrow 0$) and a negative peak corresponding to induced absorption ($v = 2 \leftarrow 1$), separated by a nodal line.

More specifically, we measure the 2D IR lineshape as a function of the waiting time, τ_2. The contours of the 2D IR spectrum change as τ_2 increases because the OH frequencies shift as molecular environments evolve (22). A distribution of frequencies that is static during τ_2 yields a lineshape that is elongated along the diagonal ($\omega_1 = \omega_3$) by the distribution of environments and broadened along antidiagonal slices [$(\omega_1 + \omega_3)/2 = \Omega$] by the dynamics of the fluctuations of molecules at frequency Ω (23). When environments interconvert on a time scale faster than τ_2, the lineshape for each resonance has a circular symmetry that reflects the statistical independence of ω_1 and ω_3. Measurements of the change in the lineshape from diagonal to symmetric as τ_2 is increased can be used to characterize the average amplitude and time scales of frequency fluctuations through a correlation function $C(t) = \langle \omega_{OH}(t)\omega_{OH}(0) \rangle - \langle \omega_{OH} \rangle^2$, but more generally reveal how one frequency evolves to another. A more detailed description of 2D IR spectra including experimental procedures can be found in Figs. 5 and 6 and *Supporting Text*, which are published as supporting information on the PNAS web site.

Fig. 2*A* displays experimentally measured 2D IR spectra of the OH stretch of HOD in D_2O for a variety of waiting times. In a broad sense the spectra evolve in a manner predicted by our previously measured frequency correlation function (21). This loss of correlation is best seen in the rotation of the nodal line separating the negative and positive peaks. At early times the lineshapes are elongated. As the waiting time increases, the node rotates, becoming nearly parallel with the ω_1 axis. The slope of the nodal line compares favorably with predictions based on our correlation function (Fig. 2*C*), which has a correlation time of 340 fs for the randomization of all OH frequencies. However, as an ensemble averaged measure of spectral fluctuations, $C(t)$ cannot distinguish dynamics of HBs and NHBs.

The asymmetry of the 2D IR lineshapes even at early waiting times is more revealing. It arises from qualitatively different spectral relaxation mechanisms for the red and blue sides of the lineshape, indicating a difference in relaxation time scales for HB and NHB species. Antidiagonal slices through the lineshape, indicated in Fig. 3*A*, demonstrate that the blue side ($\Omega_{blue} = 3{,}515$ cm^{-1}) is broader than the red side ($\Omega_{red} = 3{,}270$ cm^{-1}). The inverse line width for the blue slice is a qualitative measure

Fig. 2. Experimental and simulated 2D IR spectra of HOD in D_2O. (*A* and *B*) 2D IR correlation spectra from experiments (*A*) compared with the 2D lineshape calculated from MD simulation (*B*) for a variety of waiting times, τ_2. (*C* and *D*) Plots of the slope of the node by fitting between the fundamental and $v = 2 \leftarrow 1$ for experiment (*C*) and simulation (*D*) as a function of waiting time, τ_2. The slope of the node (squares) was calculated by fitting a straight line fit through the node of each surface between the limits $\omega_1/2\pi c = 3{,}250$ cm^{-1} to $3{,}450$ cm^{-1}. The solid line plotted with the data in *C* is the predicted behavior based on our previously measured $C(t)$ (21).
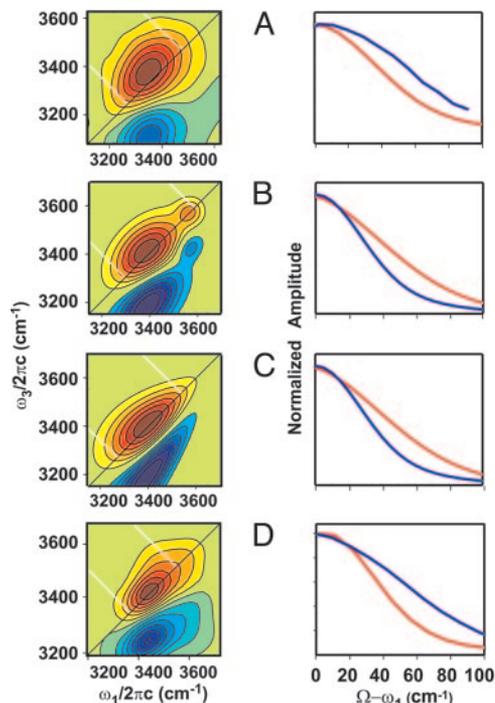
Fig. 3. Comparison of the frequency-dependent broadening of 2D IR line shapes and antidiagonal slices through 2D surfaces. The solid black line designates the diagonal axis ($\omega_3 = \omega_1$) and the white lines orthogonal to it show antidiagonal slices to the red and blue of band center. Slices were taken from each side of line center at 30% of the maximum amplitude. (*A*) Experimental data and slices for $\tau_2 = 100$ fs. (*B* and *C*) Illustrations of the predicted 2D IR line shapes and slices for two manifestations of the stable NHB model depicted in Fig. 1*B*. (*B*) A two-state model for two overlapping resonances corresponding to stable HB and NHB species. (*C*) A continuous distribution of stable species of varying hydrogen-bonding configuration. For *B* and *C*, the lineshapes were obtained by using previously established linear correlations between hydrogen-bond strength (i.e., red shift of the mean frequency relative to the gas phase) and the full width at half maximum of the OH stretching transition (24), and by including a frequency-dependent anharmonicity of the overtone transition. (*D*) The calculated 2D IR lineshape and slices as calculated from MD simulation.

of the lifetime of the NHB species and indicates that molecules initially in NHBs return to frequencies associated with HB species on the time scale of the most rapid hydrogen-bonding fluctuations (<150 fs).[††]

If NHB was a stable species as depicted in Fig. 1*B* the 2D IR lineshape would appear markedly different from the measured spectra. The well established inverse proportionality between ω_{OH} and OH line width (16, 24) can be used to predict the 2D IR lineshape for two versions of the stable NHB scenario. One consists of two stable species (Fig. 3*B*), whereas the other postulates a continuous distribution of stable species with varying hydrogen-bond strength (Fig. 3*C*). Both pictures would lead to a 2D IR lineshape at short waiting times that is preferentially broadened on the red side of the line as opposed to the blue side. The case in Fig. 3*C* most clearly matches the interpretation of

---

[††]The duration of the pulses (45 fs full width at half maximum) determines the instrumental time resolution, which is fast enough to resolve all spectral relaxations in water. Even so, the time resolution for the 2D IR experiment is not dictated by pulse length alone but by the time scales of spectral fluctuations. A finite time period $\Delta\tau$ is required to select a frequency resolution of width $\Delta\omega \approx 2\pi/\Delta\tau$. The microscopic dynamics blur the transition frequencies during $\Delta\tau$ so that the observation loses dynamic information over this interval. The shortest measurable time interval in a 2D IR experiment of the OH stretch of HOD in D_2O, determined by the inverse of the antidiagonal linewidth, is $\Delta\tau_1 + \tau_2 + \Delta\tau_3 \gtrsim$ 150 fs. This time is faster than all intermolecular motions in water except for librations.
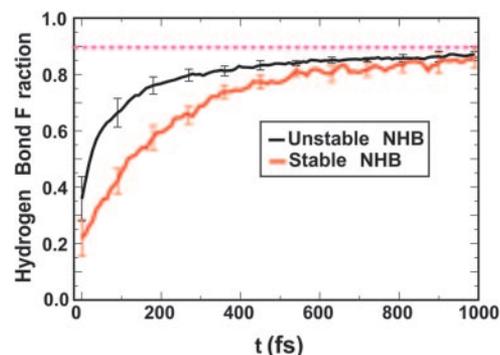

Fig. 4. Time-dependent hydrogen-bond populations at room temperature for the 7% of molecules with $\omega/2\pi c > 3{,}600$ cm^{-1} at $t = 0$. The red line identifies the small fraction (10%) of the configurations at $t = 0$ that quench into HB (stable HB), and the black line shows the configurations that quench into NHB (unstable HB). The $t = 0$ value is the fraction of stable NHB or HB that are initially hydrogen-bonded. The dotted violet line shows the equilibrium hydrogen-bond fraction (89%).

Fayer and coworkers (18, 19), who measured qualitatively similar 2D IR spectra for the OD stretch of HOD in H_2O. They concluded that time scales up to $\tau_2 = 400$ fs reflect fluctuations about relatively fixed structures, with less constrained local structures on the blue side.

MD simulations allow us to examine the microscopic origins of the 2D IR spectra in mechanistic detail (9–12). The simulation strategies we used to compute $C(t)$ for an atomistic model based on the SPC/E (simple point charge extended) pair potential (12) apply directly to calculations of 2D IR correlation spectra. Computed lineshapes, plotted in Fig. 2*B* and for comparison in Fig. 3*D*, closely resemble the corresponding experimental results in several key features. Most importantly, the blue side of the lineshape broadens along the ω_3 axis more rapidly than the red side does. The antidiagonal slices in Fig. 3*D* highlight this fact. As in the experimental measurements, the slope of the nodal line decays with a time dependence determined by $C(t)$ (Fig. 2*D*).

To determine the origins of computed spectral features in terms of hydrogen-bond dynamics, we must categorize HB and NHB. Convenient and standard geometrical criteria for identifying hydrogen bonds use only the instantaneous O-H···O distance (R_{OO}) and O-H···O angle (α) between HOD and the molecule proximal to the H atom (25). These criteria are useful for diagnosing the stability of NHBs in either of the scenarios depicted in Fig. 1 *B* and C. We designated molecular arrangements with $R_{OO} < 3.5$ Å and $\alpha < 30°$ as HBs and those with larger distances or angles as NHBs. Although these cutoff values are arbitrary, different choices do not change our conclusions.

If NHB is stable, then short trajectories initiated from this state should remain in NHB with high probability. Any barrier impeding hydrogen-bond formation will become even more pronounced if we continually remove kinetic energy from the system.[‡‡] Applied to typical H_2O or D_2O configurations, such rapid quenching produces "inherent structures" (26) of the liquid, in which $\approx$98% of the molecules donate two hydrogen bonds. These structures do not have the long-range order of ice, demonstrating that even disordered liquid environments can accommodate a saturated network of hydrogen bonds.

[‡‡]Quenching liquid configurations to nearby potential energy minima is a useful strategy for exploring basins of attraction provided the NHB state is not stabilized by entropy. An appreciable entropic contribution seems *a priori* unlikely, given the few constraints imposed by a single hydrogen bond. This expectation is confirmed by the rapid decay of NHB populations shown in Fig. 4. Details of the quenching procedure can be found in *Supporting Text*.

We applied our quenching procedure to the high-frequency distribution of molecules with instantaneous frequency >3,600 cm^{-1} (Fig. 4). Roughly 7% of the equilibrium configurations begin with ω_{OH} > 3,600 cm^{-1}. Of these, 70% begin as NHBs, but only 10% remain NHBs after quenching. We assert that only these persistent NHBs constitute broken hydrogen bonds. The remaining NHBs are not members of a separate stable state, belonging instead to the basin of attraction of intact hydrogen bonds. The fate of NHBs at ambient temperatures supports this distinction. We have classified configurations with ω_{OH} > 3,600 cm^{-1} as either stable NHBs (NHB when quenched) or unstable NHBs (HB when quenched). Fig. 4 shows how the hydrogen-bonded fraction for these two groups of configurations returns to the equilibrium fraction of hydrogen bonds (89%). The stable group clearly persists as NHBs over longer times. But even this rare collection decays quickly, with a rate of $\approx$(200 fs)$^{-1}$. These quantities demonstrate conclusively that even the most strained hydrogen bonds persist as NHBs for only a few hundred fs. Broken hydrogen bonds that persist for 1 ps or longer are extremely rare.[§§]

A typical configuration of liquid water has many instances of water molecules with apparently broken hydrogen bonds. Our experimental and theoretical results support the picture of Fig. 1*C*, in which a great majority of these NHBs are in fact just frequent excursions within the basins of attraction for hydrogen-bound molecules. Intermolecular motions, most likely librations

on the 50-fs time scale, push the NHBs into a new HB or back to the original HB. In either case, the result is a rapid red shift in ω_{OH}. Our conclusions stand in contrast to studies of water and aqueous solutions that treat various hydrogen-bonded species as chemically distinct states and examine experiments as a mixture of these hydrogen-bonded environments.

To categorize the hydrogen-bonding free energy surface, simple structural criteria used broadly in chemical and biological physics are insufficient. Our results show that neither standard geometric criteria nor the value of the OH frequency can successfully predict the fate of an NHB upon quenching. Given the failings of these classifications, we suggest that a persistence time longer than the intermolecular motion of the system should be specified to define HB and NHB species. Such a definition is taken for granted for a covalent bond, for which a stable (bound) state must persist for longer than a vibrational period. For hydrogen bonds in liquids, characterization of structure and kinetics as a function of persistence time is less common (1, 27, 28). Our results argue for a perspective originally stated several decades ago, that if NHBs are unstable, then theoretical and experimental studies of water's structure in terms of broken hydrogen bonds will "produce indecisive or contradictory results" (1). Such approaches attach a meaning to broken hydrogen bonds that should be reconsidered. For natural fluctuations at equilibrium, a broken hydrogen bond that is stabilized by liquid disorder appears to be more of a curiosity than a key player.

[§§]Simulation strategies with various different water models (9–12) and methods for computing vibrational frequencies yield qualitatively similar results for *C*(*t*). Intramolecular electronic polarizability, absent in any fixed-charge model of water, increases hydrogen bond strength and nearly doubles the value of the high-frequency dielectric constant in water. Indeed, including molecular polarizability can improve quantitative agreement between a calculated *C*(*t*) and that measured by experiment, but these effects have little bearing on our conclusions. In fact, polarizable models predict a higher degree of stabilization for HB over NHB species, further supporting our observation that presumed NHBs return back to HBs on the time scales of the fastest intermolecular motions.

1. Eisenberg, D. & Kauzmann, W. (1969) *The Structure and Properties of Water* (Clarendon, Oxford).
2. Head-Gordon, T. & Hura, G. (2002) *Chem. Rev.* **102,** 2651–2670.
3. Stillinger, F. H. (1980) *Science* **209,** 451–457.
4. Benson, S. A. & Siebert, E. D. (1992) *J. Am. Chem. Soc.* **114,** 4269–4276.
5. Robinson, G. W., Cho, C. H. & Urquidi, J. (1999) *J. Chem. Phys.* **111,** 698–702.
6. Rice, S. A. & Sceats, M. G. (1981) *J. Phys. Chem.* **85,** 1108–1119.
7. Stanley, E. H. & Teixeira, J. (1980) *J. Chem. Phys.* **73,** 3404–3422.
8. Angell, C. A. & Rodgers, V. (1984) *J. Chem. Phys.* **80,** 6245–6252.
9. Lawrence, C. P. & Skinner, J. L. (2003) *Chem. Phys. Lett.* **369,** 472–477.
10. Lawrence, C. P. & Skinner, J. L. (2003) *J. Chem. Phys.* **118,** 264–272.
11. Moller, K. B., Rey, R. & Hynes, J. T. (2004) *J. Phys. Chem. A* **108,** 1275–1289.
12. Fecko, C. J., Eaves, J. D., Loparo, J. J., Tokmakoff, A. & Geissler, P. L. (2003) *Science* **301,** 1698–1702.
13. Laenen, R., Rauscher, C. & Laubereau, A. (1998) *Phys. Rev. Lett.* **80,** 2622–2625.
14. Gale, G. M., Gallot, G., Hache, F., Lascoux, N., Bratos, S. & Leicknam, J.-C. (1999) *Phys. Rev. Lett.* 1068–1071.
15. Woutersen, S., Emmerichs, U. & Bakker, H. J. (1997) *Science* **278,** 658–660.
16. Nibbering, E. T. J. & Elsaesser, T. (2004) *Chem. Rev.* **104,** 1887–1914.
17. Yeremenko, S., Pshenichnikov, M. S. & Wiersma, D. A. (2003) *Chem. Phys. Lett.* **369,** 107–113.
18. Asbury, J. B., Steinel, T., Stromberg, C., Corcelli, S. A., Lawrence, C. P., Skinner, J. L. & Fayer, M. D. (2004) *J. Phys. Chem. A* **108,** 1107–1119.
19. Steinel, T., Asbury, J. B., Corcelli, S. A., Lawrence, C. P., Skinner, J. L. & Fayer, M. D. (2004) *Chem. Phys. Lett.* **386,** 295–300.
20. Loparo, J. J., Fecko, C. J., Eaves, J. D., Roberts, S. T. & Tokmakoff, A. (2004) *Phys. Rev. B* **70,** 180201.
21. Fecko, C. J., Loparo, J. J., Roberts, S. T. & Tokmakoff, A. (2005) *J. Chem. Phys.* **122,** 054506.
22. Hybl, J. D., Yu, A., Farrow, D. A. & Jonas, D. M. (2002) *J. Phys. Chem. A* **106,** 7651–7654.
23. Tokmakoff, A. (2000) *J. Phys. Chem. A* **104,** 4247–4255.
24. Pimentel, G. C. & McClellan, A. L. (1960) *The Hydrogen Bond* (Freeman, San Francisco).
25. Luzar, A. & Chandler, D. (1996) *Phys. Rev. Lett.* **76,** 928–931.
26. Debenedetti, P. G. & Stillinger, F. H. (2001) *Nature* **410,** 259–267.
27. Hirata, F. & Rossky, P. J. (1981) *J. Chem. Phys.* **74,** 6867–6874.
28. Sciortini, F. & Fornili, S. L. (1989) *J. Chem. Phys.* **90,** 2786–2792.